Journal of Sound and Vibration (1997) **205**(3), 323–335

A NON-LINEAR FRICTION MODEL FOR SELF-EXCITED VIBRATIONS

A. J. McMillan†

Department of Mathematics, Keele University, Staffordshire, ST5 5BG, England

(*Received* 16 *August* 1996, *and in final form* 2 *April* 1997)

The motivation behind this work is to develop a dynamical systems understanding of the phenomenon of squeal. Squeal is a form of self-excited vibration; vibrations are induced in a structure such as a wheel or violin string by the action of a frictional driving force. The nature of this force is rather difficult to define; however, a phenomenological model is proposed which combines the concepts of static and dynamic friction, which seems intuitively reasonable and for which there is documented evidence. In the case presented here, the vibrating structure is simplified to that of a block resting on a moving conveyor belt, restrained by a simple spring and dashpot to a rigid wall. The non-linear system dynamics predicted by using the new friction model are unusual in that the conditions giving rise to squeal include not only the belt speed, but also the initial conditions of the structure. It is thought that this information may be useful in the control of the onset of squeal.

1. INTRODUCTION

This research is being performed within the framework of a project concerned with the control of railway wheel squeal, the ultimate objective of which is to learn more about the onset of such vibrations, so that they may be suppressed. Railway wheels are designed to be sections through a cone, so that the effective wheel diameter may be varied by the position of the wheel relative to the track, and this provides a simple geometric differential. However, because the bogies have fixed axles, prolonged sliding of the wheel rims against the rails will occur when a train traverses a bend at speed. As the wheels slip sideways across the rails, the friction forces acting at the wheel rim excite transverse vibrations in the wheel. This is one example of friction-induced self-excited vibration, which includes the action of a bow on a violin string or a wet finger rubbed around the rim of a wine glass. It is notable that with such different structural materials and different surfaces of contact, the mechanism of vibration excitation appears so similar.

In an experimental context, the vibration of a structure known to be prone to squeal might be logged on a spectrum analyzer and the Fast Fourier Transform (FFT) of the data displayed in real time. Thus the experimentalist would see the development of the vibration of the structure from initiation to full squeal. Initially many of the vibrational modes of the structure would be excited, resulting in an FFT trace containing a number of spikes. As the vibration develops, typically one of the resonance spikes will dominate, and this increase in amplitude would indicate the incipience of squeal. A broadening of the resonance spike may also be observed, indicating a variability in the frequency.

† Present address: Transmissions Department, Rolls Royce plc., P.O. Box 31, Derby DE24 8BJ, England.

0022–460X/97/330323 + 13 $25.00/0/sv971053

In the analysis, computation of the full development of squeal would be impractical, and rather uninformative. Instead, the focus is on the behaviour of the structure at large time. To simplify the analysis as much as possible, but to retain the essential features investigated here, the vibrating structure considered is a block, attached to a rigid wall by a simple spring and dashpot. The system is driven by the frictional force between the block and the moving belt upon which it is resting: a simple one-degree-of-freedom structure with a non-linear excitation term. The configuration is shown in Figure 1. A similar analysis including a many-degrees-of-freedom model for the wheel vibration, but which uses only simple models for the friction, has been performed by Engineer and Abrahams [1].

The governing equation for this system is

$$m\ddot{x} + r\dot{x} + sx = F(\dot{x}, \ddot{x}), \tag{1.1}$$

where m is the mass of the block, s is the spring constant and r is the damping coefficient. The frictional force is given by $F(\dot{x}, \ddot{x})$, although it may be more natural to think of it as varying with time.

2. REVIEW OF FRICTION MODELS

The earliest formulation of the laws of friction was made by Leonardo da Vinci, who observed that friction seems to be independent of the area of contact, and that the frictional force is directly proportional to the applied normal load. Later, in 1781, Coulomb recognized the concept of a limiting static friction; that forces applied to a static body would not cause the body to slide unless they exceeded this limit, which is greater than the coefficient of kinetic friction. These, and the observation that the frictional force is nearly independent of the sliding speed, are generally known as Coulomb's friction law. For many purposes this is still considered to be a very good model for friction.

However, there are many instances where this model does not give predictions which have the correct quality. A particular example of this is the phenomenon of squeal. The observed phenomenon is that a small initial disturbance in a system, such as the spring–mass–damper system shown in Figure 1, can be amplified by energy transfer from the belt (or drive mechanism) to the vibrating system, even under significant levels of damping. Ultimately, the amplitude of the motion is limited; the motion increases until at one point in each cycle the velocity of the block is matched with the velocity of the belt, i.e. in a state of "stick". It is the amplification of the motion to this limit that is termed squeal, or self-excited vibration. The Coulomb friction law does not provide a mechanism for energy exchange from the belt to the spring–mass–damper system, so that in the presence of damping, initial disturbances are damped out and the long term behaviour is

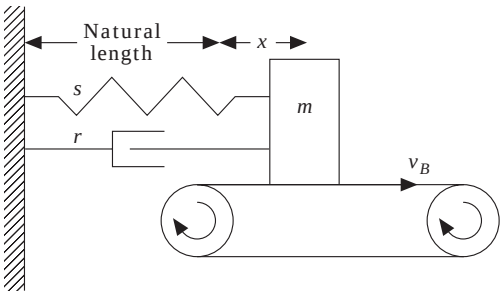

Figure 1. Friction driven spring–mass–damper system.

steady slip. The state of "stick" can be achieved only once, and then only if the initial conditions were sufficiently energetic.

It thus becomes necessary to consider the plethora of possible friction variables; each being rather complex and possibly applying in restricted circumstances. These include for example, the non-bulk material properties of the material, the surface roughness, the chemical composition of the surface, the adhesive properties of the surface, thermal properties of the surface, etc. Moreover, the frictional force will fluctuate randomly because the action of rubbing is to modify the interacting surfaces. A method of analysis based on state variables was proposed by Ruina [2], which he applied to fault motions in the Earth. This technique has also been applied by Smith [3] for the modelling of the action of the violin bow on a string. In that particular case, the important factor was the friction induced heating and the effect it has on the rosin.

The effect of many of these factors on the friction force are really understood only qualitatively and it is inappropriate to attempt to build a predictive model of friction based on such knowledge. However, it is intuitive that the precise details are largely irrelevant; Heslot *et al*. [4] concluded likewise following their experimental investigation of paper-on-paper dry-friction dynamics. What is required is a friction law which includes details which might be expected to be pertinent, and a number of parameters which may be modified, so that the model can be tuned to predict the experimental outcome for the particular regime of interest.

The phenomenon of squeal is associated with "stick-slip". This is a term first used by Bowden and Tabor [5], when describing the relative motion of two surfaces in contact. They noted that the motion is governed by a kinematic friction law while the surfaces are "slipping" and by a static law when there is no relative motion, "sticking". However, when the relative motion is very small, such as when the relative motion changes direction, it is hard to think of the kinematic and static frictions as being distinct processes. To develop a friction law which is well suited to modelling self-excited vibrations, it is thus necessary to review static and kinematic models, and bring them to a synthesis.

In the "stick" phase, the applied tangential force F_T is exactly balanced by the frictional force F. That is, the greater the applied force the greater the force due to static friction, up to a limiting value which is

$$|F_T| \leqslant F_{\max} = \mu_s mg. \tag{2.1}$$

It is only when the applied force exceeds this value that "slip" can take place. In the simplistic treatments of static friction, this limiting force is taken to be a constant, however Bowden and Tabor showed, for metal–metal contact, that junctions between the asperities on the two surfaces grow with time and applied normal force, so that bodies which have been in contact for a period of time will require a greater applied tangential force to separate them.

In the case of "slip", the effect of friction is to produce a force which opposes the direction of motion. The Coulomb friction model states that the frictional force is independent of the magnitude of the velocity

$$F = -\operatorname{sgn}(v_R)\mu_k mg, \tag{2.2}$$

where v_R is the velocity of the body against which the force F is acting, relative to the other body. However, experiments have shown that there is a velocity dependence, and Lindop and Jensen [6] demonstrated this computationally based on a qualitative understanding of surface interactions. Other authors (Ibrahim [7], Popp and Stelter [8], and Capone *et al*. [9]) have argued its significance by interpreting squeal phenomena in the light of mathematical understanding of dynamical systems. Each of these arguments leads to the

construction of a frictional force versus relative velocity graph which shows, for velocity increasing from zero, the opposing frictional force rising from zero up to a local maximum, with various behaviours as the velocity goes to infinity. The view taken by several researchers (Oden and Martins [10]) is that the variation of the friction force is due to fluctuations of the applied normal force. Kragelsky et al. [11] have reviewed the issues of friction and wear at length, and cited a number of empirical friction–velocity relationships of the form described above.

The experimental results of Wang [12] show hysteresis for relative velocities near to zero. As the relative velocity approaches zero, the frictional force rises to a local maximum and then begins to fall. It does not reach zero until the relative velocity has actually changed sign and then it finally reaches a minimum lower than the initial maximum. Sakamoto's graphs [13] show a similar phenomenon, but over a restricted range. Hunt *et al*. [14], working in 1965, also noted this effect and concluded that the frictional force was dependent on another variable besides velocity, and proposed that this be acceleration. The model presented below has been constructed to match these results qualitatively, for periodic sliding motions.

3. A PHENOMENOLOGICAL MODEL

It is well known that the elastic limit for a microscopic piece of material is far higher than for the bulk material, and the frictional contact area is comprised of many small contacts on the surface irregularities. Thus it would seem reasonable that the two contacting bodies could move a small distance relative to each other, without disrupting the temporary bonds between them, and the opposing frictional force would be predominantly due to the elastic force applied by the stretched irregularities. Such a view was proposed by Rabinowicz [15], who presented results of experiments to determine the variation of the coefficient of friction with displacement, demonstrating that the friction force quickly reaches a maximum on the length scale of the asperity height, after which it initially declines rapidly and then gradually.

It is clear that such a phenomenon would reveal itself differently depending on the relative velocity of the two surfaces, since bonds would remain unbroken for a period of time equal to the maximum extension of the bond divided by the velocity. For very low relative velocities, this time period could introduce a hysteretic effect, since the contacting bodies can move small distances relative to each other whilst remaining in a state of "stick"—a phenomenon known as "microslip". For moderate velocities the frictional force might be expected to increase in accordance with the increase of the number of bonds being broken in a time period. Obviously the random distribution and size of asperities will introduce stochastic effects which may be expected to be most significant at low relative velocities.

The sketches in Figure 2 show the motion of a block resting on a fixed slab. The block is driven relative to the slab with a velocity $v(t)$ which oscillates about zero. For high frequency oscillations with sufficiently small amplitude it is obvious that the interface between the block and the slab will remain in the "stick" phase; the strain in the bonded irregularities providing the "static" frictional force. The brush-like representation of the interface is a visualization of the growth of junctions between asperities, and the strain on these junctions. In the present work, it serves merely as an aid to intuition; however a computational model of friction, based on modelling a number of individual "bristles" has been presented by Haessign and Friedland [16].

However, if the frequency is reduced or the amplitude increased, the block will move relative to the slab by a distance greater than the maximum extension of the bonds.

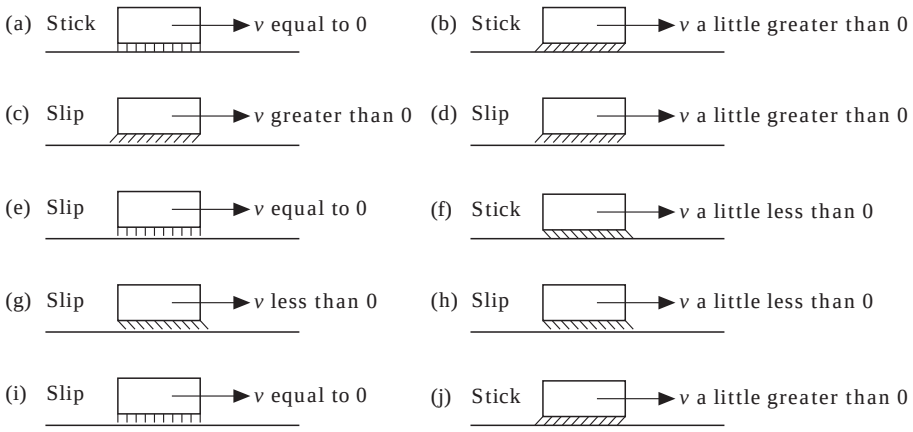

Figure 2. Schematic showing interface deformation and "stick–slip" state.

Initially, see Figure 2(a), the block is stationary and the bonds are unstrained, so that there is no force opposing the motion. In Figure 2(b), a short time later the velocity of the block relative to the belt is shown to be slightly positive, but the bonds are still intact. The frictional force opposing this motion is "static" in nature, so will rise to a limiting value. At this point, see Figure 2(c), the block begins to "slip", and at this point the frictional force becomes "kinematic", which is characterized by a sharp decrease. The block now decelerates to the slightly positive velocity where earlier it was in a state of "stick" (see Figure 2(d)) but this time it will still be slipping since the bonds have not had the time to reform. However, as the block decelerates through $v = 0$, see Figures 2(e) and (f), the bonds reform and a state of "stick" is re-obtained. The argument follows through Figures 2(g) to (j), and a frictional force–relative velocity curve is obtained (see Figure 3), which is rather similar to the one given by Wang.

If A is a typical surface irregularity size, and v_d is the greatest velocity relative to the slab at which the interface is still in a "stick" state, then one can conceive of a quantity, $\tau \sim A/v_d$, the "characteristic period" of the interface. In this work there is no attempt to measure this value, but rather to obtain an order of magnitude estimate. Typically surface irregularities are ~ 1 μm (according to Johnson [15]), and from Wang $v_d \sim 1$ mm/s. Thus $\tau \sim 10^{-3}$ seconds. For this model to be useful, the externally applied oscillations should

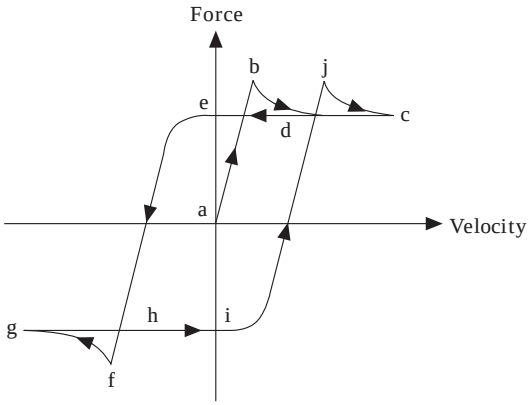

Figure 3. Schematic of frictional force versus bulk sliding velocity.

have a significantly longer period; otherwise the interface would be in a permanent "stick" state. In Wang's experiment the externally applied oscillation was 28 Hz, so it satisfies this condition. For the numerical simulation of squeal, the oscillation is governed by the vibrating structure, and will therefore have a frequency similar to that of one of the resonances.

In the interests of simplicity, it is necessary on decide to a set of variables for the friction model. For this reason, the choice has been slip velocity and acceleration. It is plausible that other effects, such as surface heating, could be linked to a combination of these, and this is almost certainly the explanation for the hysteretic effects that have been observed, i.e., slipping back onto a recently used path where new asperities may have been created and surface conditions, such as temperature, chemical composition, etc., have not yet returned to the ambient state. The problem is then to devise a function of velocity and acceleration which shows the essential features of the qualitative discussion above, i.e., which gives a curve similar to that in Figure 3.

The mathematical model proposed is presented below, generalized for the case of a block resting on a conveyor belt. Given that the belt speed is v_B, then the relative velocity of the sliding surfaces v_R is

$$v_R = \dot{x} - v_B. \tag{3.1}$$

Since the belt is taken to have constant velocity, the relative acceleration is the same as the instantaneous acceleration of the surface of the structure, $\ddot{x}$. Now, for reasonably high slip velocity the model should predict Coulomb's law, whilst for velocities close to zero stick-type behaviour should be manifest. These two types of behaviour are introduced by having two parts to the friction function,

$$F_1(\dot{x}, \ddot{x}) = -\mu_k mg(2/\pi) \arctan (v_R \mu_k / |\ddot{x}|\tau), \tag{3.2}$$

which approximates to $F_1 = \mp \mu_k mg$ for large and steady slip velocities, and

$$F_2(\dot{x}, \ddot{x}) = mg \begin{cases} -|\ddot{x}|\tau/(v_R - \ddot{x}\tau/\mu_k), & \text{if sgn } (\ddot{x}) v_R < 0 \text{ or } > 2|\ddot{x}|\tau/\mu_k \\ \text{sgn } (\ddot{x})\mu_s \sin (\Omega v_R + \Phi), & \text{otherwise} \end{cases}. \tag{3.3}$$

In these equations μ_s is a parameter which may be considered to be the analogue of the conventional coefficient of static friction. μ_k is the coefficient of kinetic friction in the Coulomb friction regime and τ is the "characteristic period" of the interacting surfaces, which determines the "width" of the quasi static friction region. In addition, $\Phi = \arcsin (\mu_k/\mu_s)$ and $\Omega = \mu_k(\pi - \Phi)/\ddot{x}\tau$. The two parts of F_2 are chosen to be continuous at $v_R = 0$ and $2|\ddot{x}|\tau/\mu_k$. For realistic values of Φ, the slope discontinuity across these points is small enough as to be imperceptible by eye. (A more complex model might insist on continuity of slope, but this probably an unnecessary luxury.) Figures 4 and 5 show F_1/mg and F_2/mg respectively, as functions of velocity with $\ddot{x} = 2\ \text{ms}^{-2}$, $\mu_k = 1$, $\tau = 10^{-3}$ s and $\Phi = 1$.

The overall frictional force is given by

$$F(v_R, \ddot{x}) = F_1(v_R, \ddot{x}) + F_2(v_R, \ddot{x}). \tag{3.4}$$

Figure 6 shows this as graph of frictional force versus relative sliding velocity for a mass sliding with sinusoidal motion, $x = 0{\cdot}5 \times 10^{-6} \sin(200t)$, relative to a surface. The shape of this graph compares well with the experimental results presented by Wang. This theoretical model was constructed to display the features of hysteresis and increased frictional force having just changed direction that were observed in the experiments. The graph in Figure 7 represents an order of magnitude lower frequency motion,

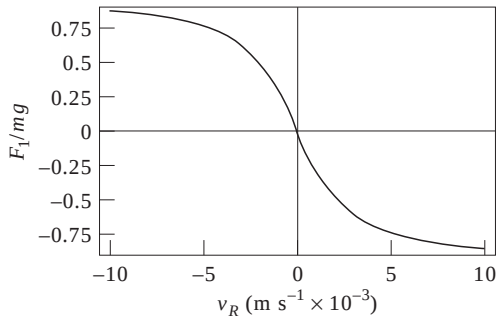

Figure 4. First part of friction function.

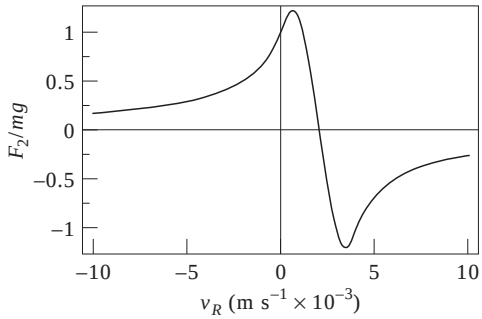

Figure 5. Second part of friction function.

$x = 5 \times 10^{-6} \sin(20t)$. This is characterized by a Coulomb type law for non-zero relative velocities, and a sharp peak very close to zero, as expected for a static law.

4. MATHEMATICAL MODEL OF THE SYSTEM

For the purposes of the present examination, a non-dimensionalized form of the governing equations will be used. Thus, without loss of generality, one may combine the equations of sections 1 and 3 to give

$$\ddot{\bar{x}} + 2\nu\dot{\bar{x}} + \bar{x} = -(2/\pi)\arctan[(\dot{\bar{x}} - \lambda/|\ddot{\bar{x}}|\bar{\tau})]$$

$$+\begin{cases} -|\ddot{\bar{x}}|\bar{\tau}/[(\dot{\bar{x}} - \lambda) - \ddot{\bar{x}}\bar{\tau}], & \text{if sgn } (\ddot{\bar{x}})(\ddot{\bar{x}} - \lambda) < 0 \text{ or } > 2|\ddot{\bar{x}}|\bar{\tau} \\ (\text{sgn } (\ddot{\bar{x}})/\sin\Phi)\sin[\{(\pi - \Phi)(\dot{\bar{x}} - \lambda)/\ddot{\bar{x}}\bar{\tau}\} + \Phi], & \text{otherwise} \end{cases}. \quad (4.1)$$

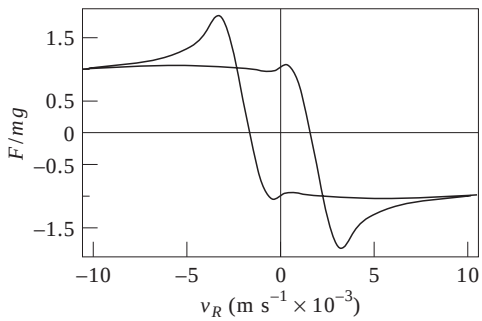

Figure 6. Friction force versus sliding velocity for sinusoidal motion at 200 rad s^{-1}.

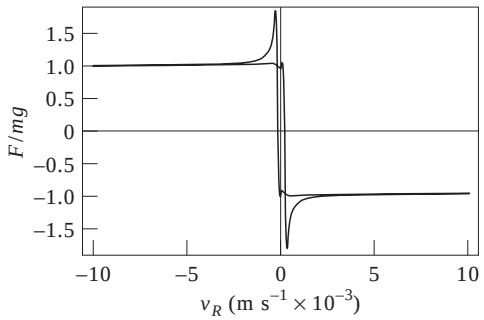

Figure 7. Friction force versus sliding velocity for sinusoidal motion at 20 rad s^{-1}.

Here $\bar{x} = (s/m)(x/\mu_k g)$ and $\bar{t} = \sqrt{s/m}\, t$ are the non-dimensionalized displacement and time respectively, $\bar{\tau} = (\tau/\mu_k)\sqrt{s/m}$ is the non-dimensionalized "characteristic period" of the interacting surfaces, and the other two independent variables are $v = r/2\sqrt{ms}$ and $\lambda = (v_B/\mu_k g)\sqrt{s/m}$. From this point the overbar notation is dropped.

The right side of equation (4.1) is the functional $F(\dot{x}(t), \ddot{x}(t))$, i.e.,

$$\ddot{x} + 2v\dot{x} + x = F(\dot{x}(t), \ddot{x}(t)). \tag{4.2}$$

If the system is started from rest at $t = 0$, that is, the forcing is zero for all $t < 0$, then it is straightforward to show that

$$x(t) = \int_0^t g(t - \grave{t})F(\dot{x}(\grave{t}), \ddot{x}(\grave{t}))\, \mathrm{d}\grave{t}, \tag{4.3}$$

where $g(t)$ is a complementary function of equation (4.2),

$$g(t) = (1/\omega)\, \mathrm{e}^{-vt} \sin(\omega t), \qquad \text{where} \qquad \omega = \sqrt{1 - v^2}. \tag{4.4}$$

Differentiating equation (4.3) with respect to t, and noting that $g(t = 0) = 0$ gives

$$\dot{x}(t) = \int_0^t \left.\frac{\mathrm{d}g}{\mathrm{d}t}\right|_{t - \grave{t}} F(\dot{x}(\grave{t}), \ddot{x}(\grave{t}))\, \mathrm{d}\grave{t},$$

and differentiating twice gives

$$\ddot{x}(t) = \int_0^t \left.\frac{\mathrm{d}^2 g}{\mathrm{d}t^2}\right|_{t - \grave{t}} F(\dot{x}(\grave{t}), \ddot{x}(\grave{t}))\, \mathrm{d}\grave{t} + \left.\frac{\mathrm{d}g}{\mathrm{d}t}\right|_{t = \grave{t}} F(\dot{x}(t), \ddot{x}(t)).$$

It is convenient to define two functions,

$$S^{(1)}(t) = \int_0^t \mathrm{e}^{-v(t - \grave{t})} \cos\{\omega(t - \grave{t})\} F(\dot{x}(\grave{t}), \ddot{x}(\grave{t}))\, \mathrm{d}\grave{t}$$

and

$$S^{(2)}(t) = \int_0^t \mathrm{e}^{-v(t - \grave{t})} \sin\{\omega(t - \grave{t})\} F(\dot{x}(\grave{t}), \ddot{x}(\grave{t}))\, \mathrm{d}\grave{t}.$$

Then,

$$x(t) = (1/\omega)S^{(2)}(t), \qquad \dot{x}(t) = S^{(1)}(t) - (v/\omega)S^{(2)}(t) \qquad \text{and}$$

$$\ddot{x}(t) = [(v^2/\omega) - \omega]S^{(2)}(t) - 2vS^{(1)}(t) + F(\dot{x}(t), \ddot{x}(t)). \tag{4.5}$$

As F is a non-linear function of $\dot{x}$ and $\ddot{x}$ these coupled integral equations cannot be solved exactly. Instead, one can recognize that they may be solved iteratively.

One assumes that $F(\dot{x}(t), \ddot{x}(t))$ may be approximated by $F(\dot{x}(t), \ddot{x}(t)) = F_j$ for $(j-1)\Delta t < t < j\Delta t$, for sufficiently small time steps Δt. Then the integrals $S^{(1)}$ and $S^{(2)}(t)$ may be written in terms of their values at previous time steps as

$$S_j^{(1)} = T_2 S_{j-1}^{(1)} - T_1 S_{j-1}^{(2)} + (T_6 + T_3)F_j \tag{4.6a}$$

and

$$S_j^{(2)} = T_1 S_{j-1}^{(1)} + T_2 S_{j-1}^{(2)} + (T_4 - T_5)F_j, \tag{4.6b}$$

where

$$T_1 = \mathrm{e}^{-v\Delta t}\sin(\omega\Delta t), \qquad T_2 = \mathrm{e}^{-v\Delta t}\cos(\omega\Delta t), \qquad T_3 = \omega\,\mathrm{e}^{-v\Delta t}\sin(\omega\Delta t),$$

$$T_4 = \omega[1 - \mathrm{e}^{-v\Delta t}\cos(\omega\Delta t)], \qquad T_5 = v\,\mathrm{e}^{-v\Delta t}\sin(\omega\Delta t), \qquad T_6 = v[1 - \mathrm{e}^{-v\Delta t}\cos(\omega\Delta t)]. \tag{4.6c}$$

T_2 is the largest of the terms, with a value of order unity. The terms T_1, T_3 and T_5 are of order Δt and the remaining two terms are negligible.

To iterate, one starts by putting $F_j = F_{j-1}$ and uses this to calculate $\dot{x}$ and $\ddot{x}$. Then one recalculates F_j based on these values. When the iteration has converged, $S^{(1)}$ and $S^{(2)}$ are reset; only the most up to date of these values need be stored. The values for F_0 and $\ddot{x}$ at $t = 0$ are calculated iteratively, based on setting the block velocity $\dot{x}(0) = 0$. In the first iteration, the block acceleration $\ddot{x}(0)$ is taken as zero.

In the model described above it has been tacitly assumed that the initial conditions of the system were, (i) that the spring was unstrained, $x(0) = 0$, and (ii) that the slip velocity was equal to the belt velocity, $\dot{x}(0) = 0$. It is clear that there are other physically possible initial conditions, and it is of interest to investigate these. Further, the results of this investigation show that the long term system dynamics are dependent on the initial conditions. The standard way to adapt the solution for non-zero initial conditions is to include two terms in the solution, with constants determined by solving the homogeneous equation with those initial conditions. However, it is rather more elegant to move to the frame of reference of the initial conditions. So, if $x(0) = x_0$ and $\dot{x}(0) = v_0$, one can write

$$\dot{x}^* = \dot{x} - v_0 \qquad \text{and} \qquad x^* = x - x_0 - v_0 t, \tag{4.7}$$

and thus obtain

$$\ddot{x}^* + 2v\dot{x}^* + x^* = F^*(\dot{x}^*(t), \ddot{x}^*(t)), \tag{4.8}$$

where $F^*(\dot{x}^*(t), \ddot{x}^*(t)) = \{F(\dot{x}(t), \ddot{x}(t)) - 2vv_0 - (x_0 + v_0 t)\}$. The problem can now be solved exactly as before, but in terms of x^* and F^*.

TABLE 1

Numerical simulation data

Symbol	λ	τ	Φ
Value	3·0	$0{\cdot}1 \times \sqrt{10}$	1·0

5. RESULTS OF THE NUMERICAL SIMULATIONS

Numerical simulations were performed on the system defined in equation (4.1), with the data given in Table 1. Various initial conditions were selected and the subsequent motions inspected. In this study interest is in the long behaviour of the system, so by using a process of trial and error, initial conditions were finally chosen so that the system quickly settled into steady behaviour.

Figure 8 shows a schematic of the type of results presented below. The outer loop represents stick–slip oscillation; the fixed point represents steady slip at constant velocity. When initial conditions are sufficiently large (in x or $\dot{x}$), the motion of the system will increase so that the trace on the phase plane will spiral out to meet it. This represents an increase in the combined energy of the system (kinetic energy in the block and potential energy in the spring). The source of this energy is the belt drive. It is transmitted to the spring–mass–damper system by the frictional force, and it is great enough to overcome the energy losses through the damper. It is important to note that this input of energy is self-limiting, and this is achieved by the friction. This has been discussed in greater detail by Heckl and Abrahams [18]. The angular frequency of motion may be estimated by dividing 2π by the number of time steps in one loop. The word "squeal" is applied in this context to suggest that the increased motion of the block would imply an increased intensity in any noise generated by the system.

If the initial conditions are close to the fixed point representing steady slip, the trace will spiral in to meet that condition. Thus the friction and the damping combine to act as a mechanism for removing energy from the system. In this case any noise generated because of initial disturbance would become softer. It is clear that there must be an unstable limit cycle which divides the initial conditions leading to the steady slip condition and those which give rise to squeal.

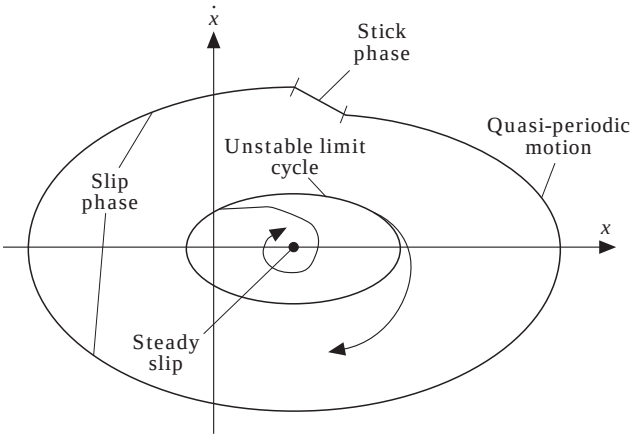

Figure 8. Schematic phase plane plot showing key features.

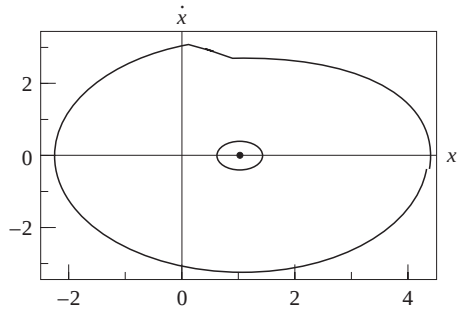

Figure 9. Phase plane plot for system with $v = 10^{-3}$.

The results presented in Figure 9 are for a system with non-dimensional damping $v = 10^{-3}$. The unstable limit cycle is rather small, and in particular, does not enclose the point (0, 0), which might be considered as the "usual initial condition". That is, if the system is started with zero spring displacement and block velocity (or any initial condition falling outside of the unstable limit cycle) oscillations will develop until at large time they spiral out to meet the outer loop. One might consider this system to be prone to squeal and stick–slip, with a frequency of about 0·96 rad s^{-1}. However, if the initial conditions are within the unstable limit cycle, then the long term behaviour will be steady slip.

The results for a similar system having damping of an order of magnitude higher $v = 10^{-2}$ are given in Figure 10. In this case the unstable limit cycle is very much larger and encloses the point (0, 0), so is prone to steady slip behaviour. However, given sufficiently energetic initial conditions it can be made to stick–slip, with a frequency of about 0·98 rad s^{-1}, and this outer loop is rather similar to that in Figure 9. Since the unforced frequency of both of these systems is 1 rad s^{-1}, the friction excitation mechanism is "pitch flattening", a phenomenon described by McIntyre and Woodhouse [16] in relation to the dynamics of bowed string instruments. The more lightly damped system is more greatly affected.

In both Figures 9 and 10 the step in the outer loop occurs when $0 < \text{sgn}(\ddot{x})(\dot{x} - \lambda) < 2|\ddot{x}|\tau$, i.e., when the relative velocity is passing though zero and the friction becomes "quasi-static". The graphs presented show only one cycle and slight discontinuities are visible where the end of the cycle does not perfectly overlap with the beginning. Subsequent cycles (not shown) have similar, but not identical paths and durations, and the position of the step can shift along the top surface. In some cycle there may be more than one step. Although the motion is not strictly periodic, it is clear that

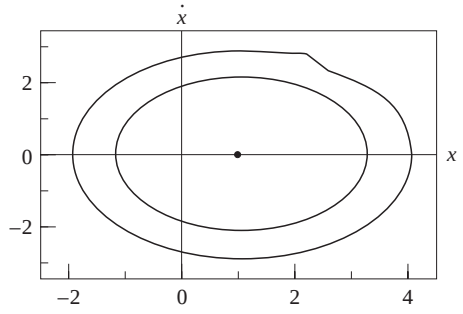

Figure 10. Phase plane plot for system with $v = 10^{-2}$.

the phase plane paths are confined to lie within a finite band, so it may be classified as "quasi-periodic". This is a consequence of hysteresis in the friction law. To understand this, consider what happens when the spring–mass–damper system has enough energy that the block can overtake the belt, the hysteresis allows this for a short period of time before the "stick" friction terms comes into play, and then energy is removed from the system. If this happens towards the left hand side of the loop, then there is still potential energy in the spring, which might be enough to accelerate the block above the belt velocity again, and cause another step within the same cycle. The location of the final step affects the amount of energy left in the system, and this determines the lower portion of the path, during which the friction law is given by the "slip" term and energy is put back into the system. The finite band would be defined by the left and right extremes of final step position.

The pronounced step feature is not observed in experiment; however, it should be remembered that friction is an inherently random process, due to the spatial variation of the surface profiles and the interaction of the surfaces (ploughing, generating new asperities, local temperature and chemcial composition fluctuations, etc.). The hysteresis in the friction model presented serves to introduce some uncertainty into timing of the "stick" phase to generate a similar effect. A more stochastic model of the "stick" term might give rise to a phase plane curve closer in shape to that observed experimentally; however, it may be rather difficult to implement computationally.

If there were no hysteresis the loop would be bounded above by the line $\dot{x} = v_B$ because there would be no mechanism for the block to exceed the belt velocity. Furthermore, once this velocity is attained, subsequent motion will be completely determined; subsequent motion is determined by the limit cycle. Thus, it may be of interest to construct a non-hysteretic friction model but with $|v_R| \gg 0$ behaviour similar to that of the model proposed above. The friction is given by

$$F(\dot{x}, \ddot{x}) = -(2/\pi)\arctan[(\dot{x}-\lambda)/|\ddot{x}|\tau] + \begin{cases} -|\ddot{x}|\tau/(\dot{x}-\lambda) & \text{if } |(\dot{x}-\lambda)| > |\ddot{x}|\tau \\ \sin[(\Phi-\pi)(\dot{x}-\lambda)/\ddot{x}\tau)]/\sin\Phi, & \text{otherwise.} \end{cases} \quad (5.1)$$

The simulation results for this shown in Figure 11 are for $v = 10^{-3}$. The unstable limit cycle is of a similar size to that in Figure 9, as might be expected, and the outer loop is flat topped, but otherwise similar to those shown in Figures 9 and 10.

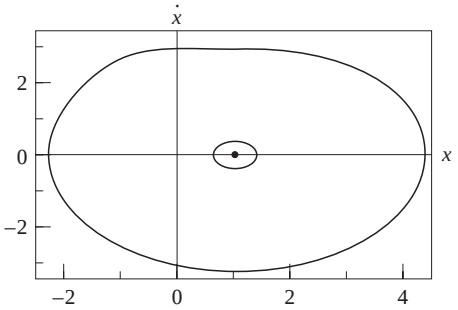

Figure 11. Phase plane plot for non-hysterical system with $v = 10^{-3}$.

6. CONCLUSIONS

In this work it has been demonstrated that if another variable besides velocity (in this case acceleration) is considered in the friction model, it is possible to see more than one type of dynamical behaviour for any given system, and that the type of long term behaviour excited will depend critically on the initial conditions.

It was previously thought that better modelling of the phenomenon of hysteresis would lead to a better understanding of the conditions required for the onset of squeal, however it seems that while hysteresis affects the nature of the stick–slip induced sound, it has little effect on the size of the unstable limit cycle which divides the stick–slip and steady slip phenomena.

ACKNOWLEDGMENTS

I would like to acknowledge the advice of I. D. Abrahams of the Department of Mathematics, Keele University, and the financial support of the EPSRC, under grant number GR/H73776. I am also grateful for constructive criticisms from the anonymous referees.

REFERENCES

1. J. C. Engineer and I. D. Abrahams (personal communication).
2. A. Ruina 1983 *Journal of Geophysical Research* **8**(B12) 10359–70. Slip instability and state variable friction laws.
3. J. H. Smith 1990 *Ph.D Thesis*, *Cambridge University*. Stick-slip vibration and its constitutive laws.
4. F. Heslot, T. Baumerger and B. Perrin 1994 *Physical Review E* **49**, 4973–4988. Creep, stick-slip, and dry-friction dynamics: Experiments and a heuristic model.
5. F. P. Bowden and D. Tabor 1964 *The friction and lubrication of solids*. Oxford University Press. See Part II, Chapter IV.
6. N. Lindop and H. J. Jensen 1997 submitted to J. de Phys. I France. Simulations of the velocity dependence of the friction force.
7. R. A. Ibrahim 1994 *Applied Mechanics Reviews* **47**, 227–253. Friction-induced vibration, chatter, squeal, and chaos part II: dynamics and modelling.
8. K. Popp and P. Stelter 1990 *Philosophical Transactions of the Royal Society of London A* **332** 89–105. Stick-slip vibrations and chaos.
9. G. Capone, V. D'Agostino, S. D. Valle and D. Guida 1992 *Meccanica* **27**, 111–118. Stick-slip instability analysis.
10. J. T. Oden and J. A. C. Martins 1985 *Computer Methods in Applied Mechanics and Engineering* **52**, 527–634. Models and computational methods for dynamic friction phenomena.
11. I. V. Kragelsky, M. N. Dobychin and V. S. Kombalov 1982 *Friction and wear*: *calculation methods*. Oxford: Pergamon Press. Translated from the Russian by N. Standen.
12. M. Wang 1994 *Doctoral Thesis*, *Technische Universität Berlin*. Untersuchungen über hochfrequente Kontaktschwingungen zwischen rauhen Oberflächen.
13. T. Sakamoto 1987 *Tribology International* **20**, 25–31. Normal displacement and dynamic friction characteristics in a stick-slip process.
14. J. B. Hunt, I. Torbe and G. C. Spencer 1965 *Wear* **8**, 455–465. The phase-plane analysis of sliding motion.
15. E. Rabinowicz 1951 *Journal of Applied Physics* **22**, 1373–1379. The nature of the static and kinematic coefficients of friction.
16. D. A. Haessig and B. Friedland 1991 *Journal of Dynamical Systems*, *Measurement and Control* **113**, 354–362.
17. K. L. Johnson 1985 *Contact mechanics*. Cambridge University Press.
18. M. A. Heckl and I. D. Abrahams 1996 *Journal of Sound and Vibration* **193**, 417–426.
19. M. E. McKintyre and J. Woodhouse 1979 *Acustica* **43**, 93–108. On the fundamentals of bowed-string dynamics.